

Influence of Reaction Time, Reducing Agent and Zinc Precursors on the Morphological Structures of Zinc Oxide

H. Shokry Hassan^{1*}, A. B. Kashyout¹, H. M. A. Soliman¹, M. A. Uosif², N. Afify³

¹Electronic Materials Researches Department, Advanced Technology and New Materials Research Institute, City of Scientific Research and Technology Applications, New Borg El-Arab City, Alexandria 21934, Egypt.

²Physics Department, Faculty of Science, Al-Azhar University, Assiut, Egypt.

³Physics Department, Faculty of Science, Assiut University, Assiut, Egypt.

*E-mail of the Corresponding author: hassan.shokry@gmail.com

Received November 13, 2013; Revised November 14, 2013; Accepted November 15, 2013

Abstract: ZnO either nanoparticles or nanorods were synthesized via sol-gel technique. Many factors were studied and optimized in order to obtain different morphological structures of nano-ZnO. Effect of reaction time (3, 6, 12, 24 and 48 hours) has been studied to optimize the best preparation condition. Reducing agent (NH₃, NaOH and KOH) is one of the factors affect on morphological structures, which has been studied in this work. Other effect has been studied in this work is zinc precursors such as Zn(NO₃)₂, ZnAc₂, ZnCl₂, and ZnBr₂. The morphological structures of prepared ZnO were revealed using scanning electron microscope (SEM) and the aspect ratios were calculated. x-ray diffraction (XRD) patterns exposed a highly crystallized wurtzite structure and used for identifying phase structure and chemical state of ZnO under different preparation conditions.

Keywords: sol-gel, morphological structures, reducing agent, SEM, preparation conditions.

Introduction

ZnO is considered as a promising material for ultraviolet light emitting diodes, laser diodes and photodetectors due to its many advanced physical properties, such as a wide band gap of 3.37 eV and a large exciton binding energy of 60 meV at room temperature, etc, Wong, E. W and Searon, P. C. (2005). Undoped ZnO is usually n-type conductive, which is associated with the presence of native point defects (e.g., oxygen vacancies (V_o) and interstitial zinc (Zn_i)) Zhang, S. B. et al (2001) or hydrogen impurities, Chris, G. and Van de Walle (2000), but the fabrication of stable and reproducible p-type ZnO has been difficult due to the self-compensation and low solubility of acceptor dopants.

These unique properties make ZnO an intriguing candidate for various optoelectronic applications including room temperature light emitting diodes, ultraviolet lasers, hydrogen storage, gas sensors and piezoelectric sensors, single-electron transistors, photo-detectors, optical modulator waveguides, varistors and solar cells, Konenkamp, R. et al (2004) & Kashyout, A. B. et al (2010).

There are several methods that have been introduced to fabricate 1D ZnO nanostructures such as wire, rod, belt, and tube including chemical vapor deposition, thermal evaporation, aqueous solution deposition, electrodeposition, template-based growth and sol-gel technique, Suh, D. I. et al (2007) & Liu Y, et al (2003).

Sol-gel processes have several advantages over other techniques for synthesizing nanopowders of metal oxides. These include the production of ultrafine porous powders and homogeneity of the product as a result of homogenous mixing of the starting materials on the molecular level.

Also, sol-gel processing holds strong promise for employment industrially on large scales, Shokry Hassan, H. et al (2013). In this work we have chosen the sol-gel technique for the previous advantages.

In this study, the effect of growth times (3, 6, 12, 24 and 48 hours) on structural and morphological characteristics of ZnO nanopowders was considered. Reducing agent (NH₃, NaOH and KOH) and zinc precursors (Zn(NO₃)₂, ZnAc₂, ZnCl₂, and ZnBr₂) were studied.

Materials and Methods

Preparation of Nanocrystalline ZnO with Different Architectures

The nanocrystalline ZnO nanopowders were prepared using sol-gel technique in the presence of different surfactants to accomplish ZnO in nanoscale with different architectures. Orthogonal experiments were carried out to determine the optimum conditions for zinc oxide nanorod formation. The major studied factors that affected zinc oxide morphology are:

- (1) Effect of zinc precursors (zinc nitrate, zinc acetate, zinc chloride, and zinc bromide).
- (2) Effect of reducing agent (ammonium hydroxide, sodium hydroxide, and potassium hydroxide).
- (3) Effect of reaction time (3, 6, 12, 24 and 48 hours).

0.3 M aqueous solution of different zinc precursors was prepared at room temperature in a glass beaker under magnetic stirring by adding the zinc salt into 250 ml of ultrapure water. 1 mol/L of reducing agent (NH₃.H₂O, NaOH or KOH) was dropped into the above-mixture till the final pH of the solution reaches to 10. The solution temperature of the solution mixture was maintained at 70 °C with 150 rpm stirring speed for different reaction times (3, 6, 12, and 24 hours). The final white powder was filtered and washed several times with alcohol and distilled water to remove any residual salts, centrifuged at 6000 rpm for 30 minutes, and then dried at 60 °C under air atmosphere.

Characterization of prepared ZnO Nanopowders

The morphological structure and the chemical compositions of the ZnO nanopowder were examined. x-ray diffraction patterns of the nanopowders were obtained using Shimadzu 7000 Diffractometer operating with Cu K α_1 radiation ($\lambda = 0.15406$ nm) generated at 30 kV and 30 mA with scan rate of 2° min⁻¹ for 2 θ values between 20° and 80°. ZnO nanopowders were investigated by scanning electron microscopy (SEM) (JEOL JSM 6360LA, Japan).

Results and Discussion

In order to attain different morphological nanostructures from the synthesized zinc oxide, the preparation conditions of zinc oxide have been varied. The variation impact of these synthesis parameters on the physical properties of the prepared zinc oxide powder are examined for optimizing the nanorod formation.

Effect of zinc precursors (zinc nitrate, zinc acetate, zinc chloride, and zinc bromide)

Variable aspect ratio (length/diameter), one dimensional ZnO nanostructures are synthesized by reacting Zn²⁺ precursor derived from Zn.(NO₃)₂, Zn.Ac₂, Zn.Cl₂, and Zn.Br₂ via sol-gel technique. This

section deals with a simple study on the relationship, between the reaction conditions with Zn^{2+} ions derived from different precursors and their morphologies. The nucleation and growth mechanisms for different architecturing ZnO will be discussed according to their characterizations that include powder scanning electron microscopy (SEM) and x-ray diffraction (XRD).

Scanning electron microscope (SEM)

(Figure1) shows the scanning electron micrographs of ZnO which has been prepared using different zinc precursors in presence of the most proper surfactant of PEG with M.wt=400. Zinc nitrate, zinc acetate, zinc chloride, and zinc bromide were used as starting materials for producing different zinc oxide configurations. It is noted that, ZnO formed using either $Zn(NO_3)_2$, $ZnCl_2$, or $ZnBr_2$ has nanorod configuration, however that produced using $ZnAc_2$ has hexagonal particles morphology. The ZnO nanorods formed in presence of either $ZnCl_2$ or $ZnBr_2$ exhibits a wide size distribution except the case of $Zn(NO_3)_2$ that produce a uniform size distribution of flower-like nanorod ZnO aggregates. This observation gives a prediction that $Zn(NO_3)_2$ is the most preferred starting material for production of uniform ZnO nanorods. The length of rods formed in the case of $ZnCl_2$ is in range (200-900 nm) and the diameter size is from 100-200 nm as shown in fig.1b. The average length and diameter of the nanorods was estimated to be 550 nm and 150 nm respectively (figure.1c). The average aspect ratio of ZnO prepared using $ZnCl_2$ is about 3.6. However, For $ZnBr_2$ precursors the produced ZnO nanorods have the length range between (250-2500 nm) and diameter range of (200-400 nm) with average aspect ratio of 4.6 (figure.1d). The hexagonal ZnO nanorods formed in presence of $Zn(NO_3)_2$ as a precursors have average length and diameter around 2000 and 150 nm respectively, and approximately aspect ratio is more than 13 (figure.1a). So, it is concluded that the precursor composition has determinative effects on ZnO formation, Wang, H. et al (2011). It is generally believed that crystal formation of ZnO in solutions can be divided into two stages; crystal nucleation and growth as discussed previously. The effective reason for the precursor affecting the morphology of ZnO could be attributed to different reaction pathways, solubility of the precursor, and basicity of the solution which influenced the crystal nucleation and growth, Tak, Y and Yong, K. (2005), Cho, S. et al (2008) & Arca, E. et al (2009). When the growth rate dominates over the nucleation rate, the crystallite size increases, while in the case of nucleation domination the crystallite size decreases, Rajeswari, N. et al (2011). This explains the case of zinc nitrate, zinc chloride and zinc bromide precursors, where in these cases the growth rate is dominated over the rate of nucleation that tends to form ZnO with nanorod structures as investigated in (figure1). However, the ZnO deformation mechanism was inverted for zinc acetate precursor, where the nucleation rate is relatively high than the rate of growth. This creates great amounts of ZnO nuclei and limiting the crystal growth rate, and then large-scale of hexagonal ZnO particles were produced. The similarity of ZnO morphology (nanorods) produced from either zinc nitrate, zinc chloride or zinc bromide precursors may be owing to their near similar basicity. Where they produce intermediate by products of strong acids of HNO_3 , HCl and HBr respectively in contrast to the weak acetic acid formed in the case of zinc acetate precursor, Gao, X. D. et al (2005), Özgür, Ü. et al (2005).

Accordingly, the most proper zinc precursor is that produces a uniform size distribution of ZnO nanorods with high aspect ratio is selected to be zinc nitrate.

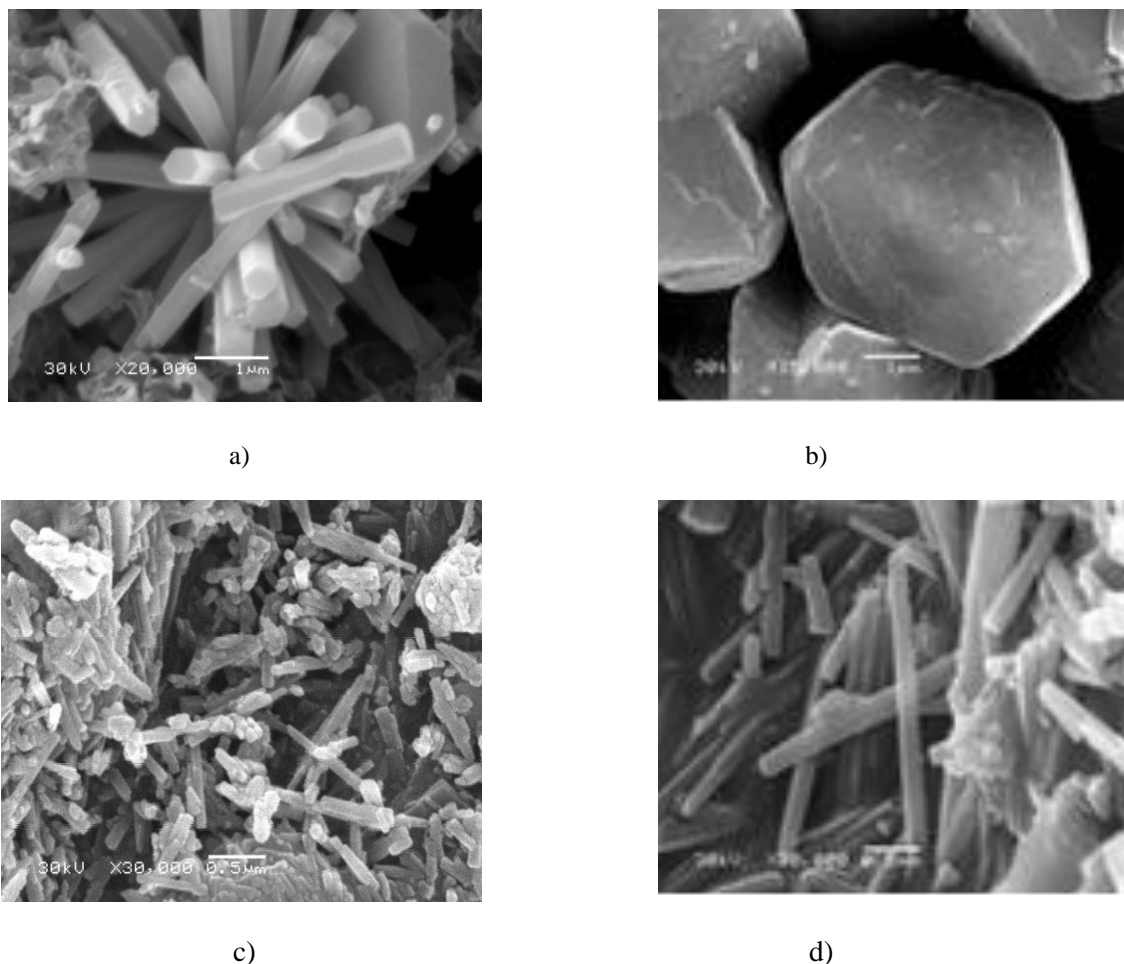


Figure1. SEM Micrographs for different precursors of Zinc: (a) Zinc nitrate (b) Zinc Acetate, (c) Zinc Chloride, (d) Zinc Bromide.

X-Ray Diffraction Analyses

The standard XRD patterns of the different produced ZnO are used for relative comparison of crystal structures for the ZnO nanopowders, prepared using different precursors as shown in (figure 2). The as-synthesized ZnO nanopowders produced diffraction patterns and all are well indexed as crystalline hexagonal phase wurtzite structure which can be indexed to (JCPDS card No. 01-089-0138). No peak attributable to possible impurities is observed. The sharp diffraction peaks manifest that the as-prepared ZnO nanostructures have high crystallinity, Makkar Meenu and Bhatti, H. S. (2011).

The calculated lattice constants of the prepared ZnO using sol-gel technique in presence of different zinc precursors are illustrated in (table 1) and compared with the reference lattice constants of wurtzite ZnO ($a=0.3253$ nm, $c=0.5213$ nm, $u=1.6025$).

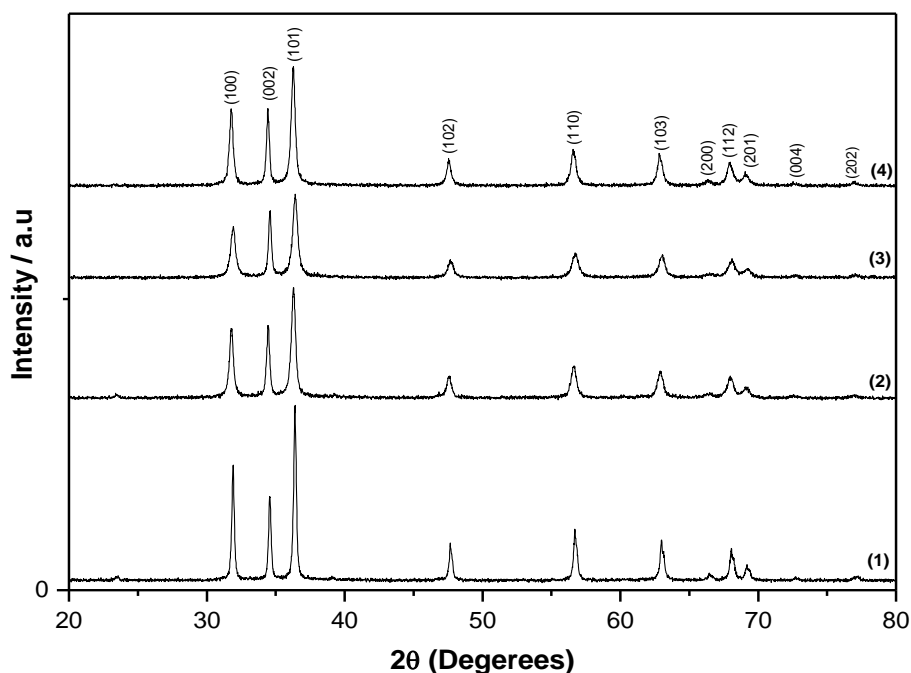


Figure 2. XRD Patterns for ZnO nanopowders prepared using different precursors; (1) Zinc Nitrate, (2) Zinc Acetate, (3) Zinc Chloride, (4) Zinc Bromide.

It is concluded from this table that ZnO lattice constants follow the zinc precursor sequence of zinc chloride < zinc nitrate < zinc bromide < zinc acetate. This sequence may be regarded to their basicity that follows the same sequence. These results are predicted from the previous studied ZnO morphology. Where both zinc chloride, zinc nitrate and zinc bromide produced a nonrods structural except zinc acetate that produced hexagonal particles.

Table1. Lattice Constants Measurements for Different Zinc Precursors

Zinc precursor	Lattice Constant [a] direction (nm)	Lattice Constant [c] direction (nm)	Lattice ratios c/a
Zn(NO ₃) ₂	0.3499	0.52	1.486
ZnAc ₂	0.3501	0.5206	1.487
ZnCl ₂	0.3489	0.5187	1.487
ZnBr ₂	0.3503	0.5208	1.487

Effect of reducing agent (ammonium hydroxide, sodium hydroxide, and potassium hydroxide)

It is evidence that the role of pH value of the reaction mixture has a significant role in ZnO formation. In order to elucidate whether the alkaline source that used for pH justification has a role in the formed ZnO or only the pH value of the reaction mixture is the limiting factor regardless of the type of alkaline source. So, different reducing agents of NaOH, KOH, and NH₃ are used to adjust the reaction pH at pre-determined optimum value of 10.

Morphological Structure (SEM)

It is specified from the previously studied ZnO preparation parameters, that the most preferred ZnO produced has a flower-like nanorod structure. So, the preparation conditions that produce this structure are specified as the optimum conditions.

Accordingly, $Zn(NO_3)_2$ is used as a starting precursor in presence of PEG (400 Mwt) surfactant at the pH value of the reaction mixture was justified at 10 using 1M solution of different alkaline sources of NaOH, KOH, and NH_3 , Lili, Wu, et al (2005). The SEM images of the produced ZnO are investigated in (figure 3). The morphology of ZnO powders synthesized using strong alkaline reducing agent of either NaOH or KOH produces elongated hexagonal nanoparticles with average aspect ratios about 2.

However, when weak alkaline reducing agent of NH_3 was used, the elongated hexagonal particle was transformed into flower-like nanorod morphology. For strong alkaline reducing agent (NaOH, KOH), a large number of $Zn(OH)_4^{2-}$ species which act as seeds for the formation of ZnO are formed, that by its rule decrease the growth rate for ZnO formation, Naghmeh Faal Hamedania, et al (2011).

Subsequently, the anionic PEG species produce negative electrostatic interactions with the negative polar plane of $Zn(OH)_4^{2-}$ seeds. This clearly directs $Zn(OH)_4^{2-}$ species to assure oriented growth randomly for ZnO leading to form elongated particles. These results indicate that, the reducing agent with weak alkalinity (NH_3) is most preferable for ZnO formation with flower-like nanorod morphological structure.

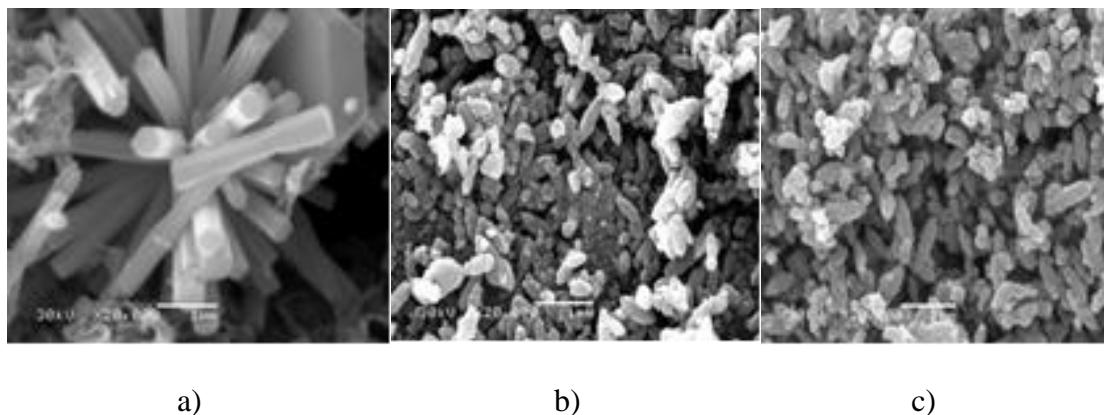


Figure 3. SEM Micrographs for Different Reducing Agents: (a) NH_3 (b) NaOH, (c) KOH.

X-Ray Diffraction Analyses

Comparing the x-ray diffraction (XRD) patterns of the different produced ZnO powders using 1M aqueous alkaline solution of the different reducing agents is shown in (figure 3).

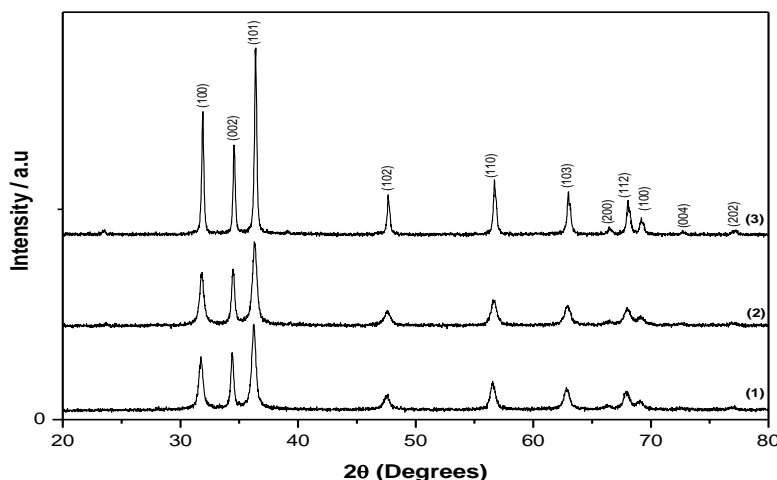


Figure 4. XRD Patterns for ZnO nanopowders prepared with different reducing agents; (1) NaOH, (2) KOH, (3) NH₃.

It is clearly revealed the formation of stable monophasic ZnO with a hexagonal (wurtzite-type) crystal structure for the different studied alkaline sources. Moreover, the XRD patterns indicated that ZnO powders synthesized using various alkaline sources possess preferred orientation along different crystallographic planes. However, it is clear that the degree of crystallinity of formed ZnO in case of using weak alkaline reducing agent of NH₃ (figure.4(1)) is improved compared with that produced using strong alkaline reducing agent of either NaOH or KOH. So, ammonia solution as reducing agent is preferable for producing ZnO with high crystallinity.

(Table 2) illustrates the fact that with increasing strength of the reducing agent, lattice spaces are increased. Accordingly, for the weak reducing agent (NH₃), the lattice constants of formed ZnO are relatively small and their values are close to that of the wurtzite ZnO reference. The overall conclusion from both SEM & XRD results is that the ammonia solution is the most suitable reducing agent to be utilized for production highly crystalline ZnO in flower-like nanorod structure.

Table.2. Lattice Constants Measurements for Different reducing agents.

Reducing agent	Lattice Constant [a] direction (nm)	Lattice Constant [c] direction (nm)	Lattice ratios c/a
NH ₃	0.3499	0.52	1.486
NaOH	0.3499	0.5205	1.487
KOH	0.3502	0.5207	1.487

Effect of Reaction Time on Zinc Oxide Formation

The reaction time of the reaction mixture at the pre-determined optimum conditions of Zn (NO₃)₂ precursor in presence of PEG (400 Mwt) surfactant adjusting the pH of the reaction mixture at value 10 using ammonia solution was varied in the range of (3, 6, 12, 24, and 48 hours).

Morphological Structure (SEM)

SEM images of the ZnO structures at various reaction times of 3, 6, 12, 24, and 48 h, respectively are shown in (figure. 5). It is clear that the ZnO nanostructures depended on the growth time, where different morphological structural of nanoparticles, nanorods and flower-like rods architectures can be seen. For short growth periods of 3 and 6 hours (figure. 5 a, b), aggregate nanoparticle structures are indicated. These aggregated particles suggested to be the Zn(OH)₂ microcrystals.

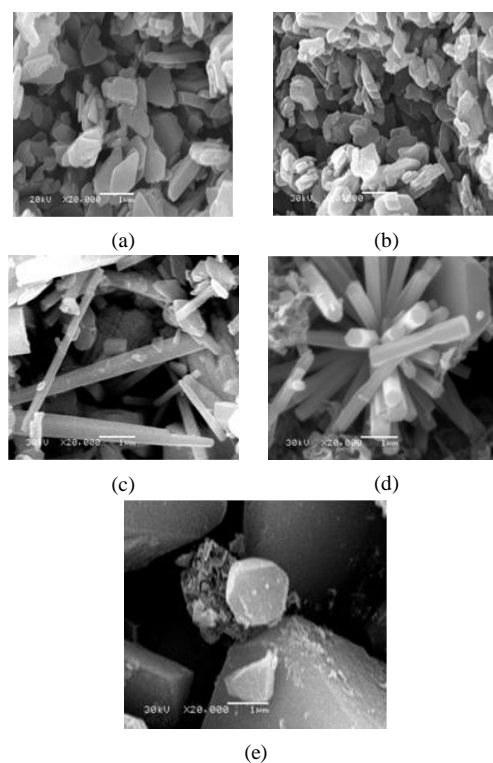


Figure 5. SEM Micrographs for different reaction time: (a) 3 (b) 6, (c) 12, (d) 24, (e) 48 h.

As the reaction period increased above 6 h, the nanoparticles disappeared and nanorod architectures of ZnO can be achieved. The absence of nanoparticles is consistent with the fact that the Zn(OH)₂ is acting as a reservoir, maintaining the Zn²⁺ concentration well below that where nucleation can occur Ruth, A. et al (2003). However, for growth time of 24 hours, well-formed flower-like nanorod structures have been predominated. The suggesting mechanism for ZnO may be considered As the ZnO nanorod-like structure are formed from the decomposition of Zn(OH)₂ within 60 minutes heating, after that, the following time growth of the particles must result from a dissolution and re-precipitation of the existing ZnO particles. The results suggest that this is a slow process, as significant changes in the particle dimensions are only seen after 6 hours ageing. As, the reaction time increased above 24 hours, the formed nanorod structure of ZnO was converted to nanoparticles. That may be due to the increase in the stirring period of the formed ZnO rods after 24 h, destroy the initial oriented growth chain of ZnO that lead for rod formation to form ZnO with hexagonal nanoparticle shapes. Subsequently from

the SEM results, the most reaction time for ZnO formation in nanorod structural with high aspect ratio was 24 hours.

X-Ray Diffraction Analyses

(Figure 6) shows XRD patterns for ZnO nanopowder that was prepared using different reaction times. All the diffraction peaks can be indexed as the hexagonal wurtzite structure with high crystallinity except that produced at short time intervals of 3, and 6 hours as shown in (figure.6-1, 2). Where, at these reaction time, the characteristic peaks can be indexed as Zn(OH)₂ (JCPDS card No. 01-089-0138).

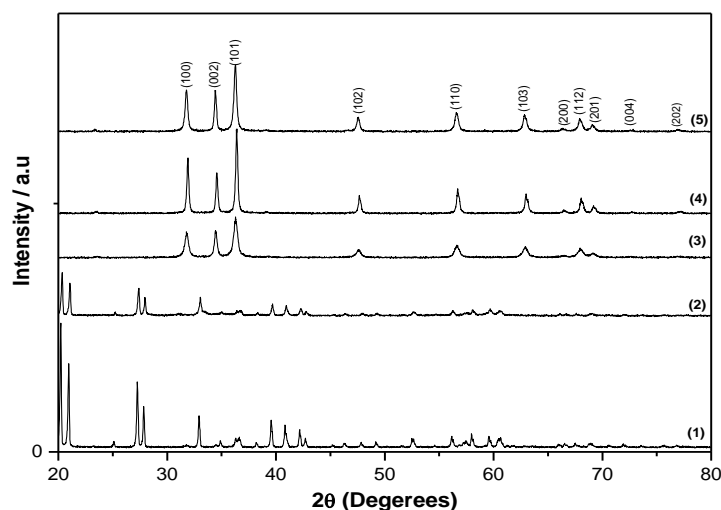


Figure 6. XRD Patterns for ZnO nanopowders prepared with different reaction times; (1) 3, (2) 6, (3) 12, (4) 24, (5) 48 hours.

This may be regarded to the insufficient reaction time to convert the intermediate Zn(OH)₂ complex to form ZnO as previously mentioned in the previous SEM discussion. As the reaction time increased above 6 hours (figure 6-3, 4, 5), the rate of Zn(OH)₂ complex decomposition tend to be completed. Where no impurity peaks has been detected from their XRD spectrum, which means that the entire crystalline precursors have decomposed and grew into ZnO single crystals. Moreover, it is clear that the increase in the reaction time improve the degree of crystallinity of the formed ZnO. These results are compatible with outcome of Ruth A. McBride and others (2003), who has studied the effect of reaction time on ZnO crystalline structure using hydrothermal process.

The calculated lattice spaces of produced ZnO are compared with wurtzite structure of ZnO and illustrated in (table 3). It is observed that, as the reaction time increased, the ZnO lattice constants are decreased and their values tend to be equal with that of comparable ZnO wurtzite structure. This may be related to; as the reaction time increased, the rate of Zn(OH)₄²⁻ complexes decomposition forward to its complete that has large values of lattice constants and its presence affect in the lattice constants of the produced ZnO. Once the reaction time reached to 24 h, ZnO formation attains to maximum capability of formation and Zn(OH)₄²⁻ complexes disappear. These results confirm both SEM and XRD results. Consequently, the optimum time of reaction for ZnO formation with high degree of crystallinity was selected to be 24 hours.

Table 3. Lattice Constants Measurements for Different Reaction Times.

Reaction time (h)	Lattice Constant [a] direction (nm)	Lattice Constant [c] direction (nm)	Lattice ratios c/a
6	0.35	0.5204	1.487
12	0.35	0.5203	1.487
24	0.3499	0.52	1.486
24	0.3503	0.5208	1.487

Conclusions

In the present work, ZnO nanopowders have been investigated successfully in different architectures (nanoparticles, elongated particles and nanorods). The factors which control the formation of ZnO nanopowders via sol-gel technique were optimized in order to acquire ZnO that have nanorod morphological structure with high aspect ratio. According to the characterization results of the different ZnO synthesized nanopowders that produced from the different studied preparation conditions, through analyzing the preparation results, the following conclusions can be established; Zinc nitrate was proved to be the most preferred starting material for producing uniform size distribution ZnO nanorods that has flower-like nanorod aggregates with high degree of crystallinity. 24 hour was specified as the optimum reaction time for ZnO formation with high degree of crystallinity in nanorod structure. Ideal reducing agent to obtain high degree of crystallinity and uniform size size distribution ZnO nanorods was NH_3 .

Acknowledgment

The authors gratefully acknowledge Dr. Marwa Farouk Elkady for her role and contribution in this work.

References

1. Arca, E. and Fleischer, K. Shvets, I.V. (2009). influence of the Precursors and Chemical Composition of the Solution on the Properties of ZnO Thin Films Grown by Spray Pyrolysis, *J. Phys. Chem. C* 113, p.21074-21081.
2. Cho, S. Jung, S. H. Lee, K. H. (2008). Morphology-Controlled Growth of ZnO Nanostructures Using Microwave Irradiation: from Basic to Complex Structures, *J. Phys. Chem. C* 112, p.12769-12776.
3. Chris, G. Van de Walle. (2000). Hydrogen as a cause of doping in zinc oxide. *Phys. Rev. Lett.* 85, p. 1012.
4. Gao, X. D, Li, X. M. and Yu, W. D. J. (2005). *Solid State Chem.* 178, 1140.
5. Kashyout, A. B, Soliman, H. M. A, Shokry Hassan, H. and Abousehly, A. M. (2010) Fabrication of ZnO and ZnO:Sb Nanoparticles for Gas Sensor Applications, Article ID 341841, 8 pages.
6. Konenkamp, R. Word, R. C. Schlegel, C. (2004). Vertical nanowire light-emitting diode. *Appl. Phys. Lett.* 85. P. 6004–6006.
7. Lili Wu, Youshi Wu, Wei Lu, Huiying Wei, Yuanchang Shi. (2005). Morphology development and oriented growth of single crystalline ZnO nanorod, *Applied Surface Science* 252, p. 1436-1441.

8. Liu Y, Chu Y, Li L. L, et al. (2003). Controlled fabrication of highly oriented ZnO microrod/microtube arrays on a zinc substrate and their photoluminescence properties, *Chem Eur J*, 15, P. 6667-6683.
9. Makkar, Meenu and Bhatti, H. S. (2011). Inquisition of reaction parameters on the growth and optical properties of ZnO nanoparticles synthesized via low temperature reaction route, *Chemical Physics Letters*. 507, 29, p.122-127.
10. Naghmeh Faal Hamedani, Ali Reza Mahjoub. Abbas Ali Khodadadi, Yadollah Mortazavi, (2011). Microwave assisted fast synthesis of various ZnO morphologies for selective detection of CO, CH₄ and ethanol, *Sensors and Actuators B: Chemical*, 156, P. 737-742.
11. Özgüra, Ü., Alivov, Ya., I. Liu, C., Tekeb, A., Reshchikov, M. A., Doğanc, S., Avrutin, V. Cho, S. J. and Morkoç, H. (2005). A comprehensive review of ZnO materials and devices, *J. Appl. Phys.* 98, 041301-103.
12. Rajeswari Yogamalar, N., and Arumugam Chandra Bose, (2011). Tuning the aspect ratio of hydrothermally grown ZnO by choice of precursor, *Journal of Solid State Chemistry*. 184, 1, p.12-20.
13. Ruth A. McBride, John M. Kelly, and Declan E. McCormack. (2003). Growth of well-defined ZnO microparticles by hydroxide ion hydrolysis of zinc salts, *J. Mater. Chem.*, 13, p.1196-1201.
14. Shokry Hassan, H., Kashyout, A.B., Soliman, H. M. A., Uosif, M. A., Afify, N., (2013). Effect of reaction time and Sb doping ratios on the architecturing of ZnO nanomaterials for gas sensor applications. *Applied Surface Science* 277. p.73-82.
15. Suh, D. I. Lee, S. Y. Kim, T. H. Chun, J. M. Suh, E. K. Yang, O. B. Lee, S. K. (2007). The fabrication and characterization of dye-sensitized solar cells with a branched structure of ZnO nanowires. *Chem. Phys. Lett.* 442, p. 348-353.
16. Tak, Y., Yong, K., (2005). Controlled growth of well-aligned ZnO nanorod array using a novel solution method, *J. Phys. Chem. B* 109, p.19263-19269.
17. Wang, Hu., Xie, Juan., Yan, Kangping., and Ming, Duan, (2011). Growth Mechanism of Dierent Morphologies of ZnO Crystals Prepared by Hydrothermal Method, *J. Mater. Sci. Technol*, 27(2), 153–158.
18. Wong, E. W. Searon, P. C. (2005). p-type behavior in In–N codoped ZnO thin films. *Applied Physics Letters* 87, 252106.
19. Zhang, S. B., Wei, S. H., Zunger, A. (2001), Intrinsic n-type versus p-type doping asymmetry and the defect physics of ZnO, *Phys. Rev. B* 63 p.75-205.